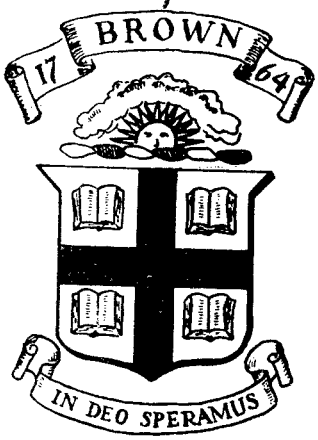

Division of Engineering
BROWN UNIVERSITY
PROVIDENCE, R. I.

AN ANALYSIS OF COMBINED LONGITUDINAL AND TORSIONAL PLASTIC WAVES IN A THIN-WALLED TUBE

BY

R. J. CLIFTON

Department of Defense
Advanced Research Projects Agency
Contract DA-19-020-AMC-0077(R)
ARPA Order No. 71
Supervised by Ballistic Research Laboratories
Aberdeen Proving Ground

Report No. 5

May 1966

AN ANALYSIS OF COMBINED LONGITUDINAL AND TORSIONAL PLASTIC WAVES IN A THIN-WALLED TUBE

by

R. J. Clifton

Technical Report No. 5
Division of Engineering
Brown University
Providence, Rhode Island

May 1966

Sponsored by
Department of Defense
Advanced Research Projects Agency
under Contract DA-19-020-AMC-0077(R)
ARPA Order No. 71, supervised by
Ballistic Research Laboratories
Aberdeen Proving Ground

An Analysis of Combined Longitudinal and Torsional Plastic Waves in a Thin-Walled Tube[1]

by

R. J. Clifton[2]

Abstract. This paper presents a one-dimensional rate independent theory of combined longitudinal and torsional plastic wave propagation in a thin-walled cylindrical tube. The tube material is assumed to behave as an isotropic work-hardening, elastic-plastic solid, for which the stress-strain curve in simple tension is a smooth curve, concave toward the strain axis. The resulting equations are shown to yield two wave speeds, c_f and c_s, which satisfy the inequalities $c_2 \leq c_f \leq c_o$ and $c_s \leq c_2$ where c_2 is the elastic shear wave velocity and c_o is the elastic bar velocity. The solution is given for combined longitudinal and torsional step loading of a semi-infinite tube, which is initially at rest and either unstressed or statically pre-stressed to arbitrary values of normal stress and shear stress. The solution consists of adjoining centered simple wave solutions and constant state solutions. There are two types of simple wave solutions corresponding to the two wave speeds c_f and c_s. The stress paths in stress-space associated with these two types of simple waves form an orthogonal network.

---

[1] This research was partly supported by the Department of Defense Advanced Research Projects Agency, Order No. 71, through Contract DA-19-020-AMC-0077(R) with Ballistic Research Laboratories, Aberdeen Proving Ground, Maryland. Partial support was also provided by the Advanced Research Projects Agency under Contract SD-86.

[2] Assistant Professor of Engineering (Research), Brown University, Providence, Rhode Island.

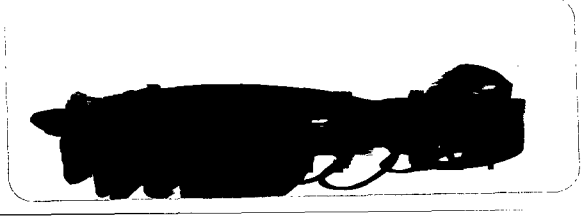

Introduction

A test involving combined dynamic stress states which is attractive from the point of view of analysis and which would not seem to present unsurmountable experimental difficulties is that of combined longitudinal and torsional impact of a thin-walled cylindrical tube. Such a test, for stress states beyond the elastic limit of the material, could be expected to provide useful information regarding the dynamic plastic behavior of solids under combined stress states. Clearly this information is of fundamental importance in the development of a three-dimensional theory of plastic wave propagation. In order to interpret the results of plastic wave tests, designed to study the dynamic mechanical behavior of a material, it is necessary to first solve the associated boundary value problem for an assumed material behavior; the appropriateness of the assumptions regarding the material behavior is then evaluated by comparison of theory and experiment. Accordingly, the purpose of this paper is to present an analysis of combined longitudinal and torsional impact of a thin-walled cylindrical tube, based on an assumed material behavior which, although simple, could be expected to result in a useful theory for interpreting experimental observations. It will be assumed that the stress-strain curve for simple tension is smooth, concave toward the strain axis, and independent of the rate of strain; that the material satisfies either the Tresca or von Mises yield conditions; that isotropic work-hardening applies; that the elastic and plastic strain rates are separable and that the plastic strain rate is given by the theory of the plastic potential. In other words, the theory is the same as the usual quasi-static, elastic-plastic theory for isotropic work-hardening (see e.g. [1]) except that the inertia terms are included.

The theory presented here reduces to that of von Kármán [2] for the case of longitudinal impact, without torsion. It is similar to the theory presented

by Bleich and Nelson [3] for the case of a uniformly distributed step load of pressure and shear on a half space, except that Bleich and Nelson assumed the material to be elastic-perfectly plastic. Rakhmatulin [4] and Cristescu [5] have used a deformation theory of plasticity to study elastic-plastic wave propagation for combined stress states analogous to the stress states considered here. They considered the case of edge impact of two plates for which the directions of the velocities of the two plates are in the plane of the plates and are oblique to the impacting faces; for their case the normal strain in the direction parallel to the impacting faces and in the plane of the plates is zero whereas in the case considered here the normal stress in the corresponding direction is assumed to be zero. Rakhmatulin described a solution in which first a uniaxial stress state propagates into the body as a simple wave followed by a constant state; then a combined stress state propagates as a wave of strong discontinuity followed by a constant state. Cristescu, using the same equations as Rakhmatulin and assuming a material for which the slope of the stress-strain curve in shear is less than the secant modulus, found two types of combined stress waves. He showed that a given level of compressive strain propagates faster in the faster of these two combined stress waves than it would in a plastic wave for a uniaxial stress state; similarly, in the slower combined stress wave the velocity of propagation of a given level of shear strain was shown to be faster than in a plastic wave of pure shear. From these results Cristescu concluded that combined dynamic stress is transmitted in a body only by combined stress waves. In contrast with the results of Rakhmatulin and Cristescu, the present theory predicts that a wave of strong discontinuity occurs only in elastic regions and that a leading uniaxial plastic wave exists for a step load of normal stress and shear. A bibliography of studies of one-dimensional plastic waves involving combined stress states is given in a survey paper by Cristescu [6].

1. Derivation of the Basic Equations

Consider a long slender thin-walled tube with mean radius $\bar{r}$ as shown in Fig. 1. Let $U(x,t)$ denote the average displacement in the longitudinal direction at time t of the cross-section at a distance x from the impact end of the tube. Since this is to be a small deformation theory, the coordinate x can refer to either the initial position of the cross-section or its position at time t. Let $\varepsilon(x,t)$ denote the longitudinal strain U_x, (subscripts x and t denote partial differentiation with respect to x and t respectively) and $u(x,t)$ the longitudinal particle velocity U_t. Then if U is twice continuously differentiable

$$\varepsilon_t = u_x \tag{1}$$

Analogously, let $\Omega(x,t)$ denote the average rotation about the x-axis at time t of the cross-section at x. Let $\gamma(x,t)$ denote the shearing strain $\bar{r}\Omega_x$, and $v(x,t)$ the tangential velocity $\bar{r}\Omega t$. Then, neglecting changes in $\bar{r}$, we have

$$\gamma_t = v_x \tag{2}$$

Conservation of linear momentum gives

$$\sigma_x = \rho u_t \tag{3}$$

where $\sigma(x,t)$ is the force in the longitudinal direction per unit cross-sectional area and ρ is the density. Conservation of angular momentum gives, again neglecting changes in $\bar{r}$,

$$\tau_x = \rho v_t \tag{4}$$

where $\tau(x,t)$ is the force in the tangential direction per unit cross-sectional area.

The strain rates ε_t and γ_t are assumed to be the sum of an elastic part and a plastic part.

Thus,

$$\varepsilon_t = \varepsilon_t^e + \varepsilon_t^p \tag{5a}$$

$$\gamma_t = \gamma_t^e + \gamma_t^p \tag{5b}$$

where the superscripts e and p denote the elastic and plastic parts respectively. In formulating the stress-strain relations it will be assumed that σ and τ are the only non-zero stresses; in particular, the hoop stress associated with the lateral inertia of the tube will be neglected. For an isotropic elastic solid the elastic parts in Eqs. (5) are given by

$$\varepsilon_t^e = \frac{1}{E}\,\sigma_t \tag{6a}$$

$$\gamma_t^e = \frac{1}{\mu}\,\tau_t \tag{6b}$$

where E is Young's modulus and μ is the modulus of rigidity.

The plastic strain rates are given by

$$\varepsilon_t^p = \dot{\lambda}\,\frac{\partial f}{\partial \sigma} \tag{7a}$$

$$\gamma_t^p = \dot{\lambda}\,\frac{\partial f}{\partial \tau} \tag{7b}$$

where $f(\sigma,\tau)$ is the yield function and $\dot{\lambda}$ is a positive scalar function to be specified subsequently. The yield condition is assumed to have the form

$$f(\sigma,\tau) \equiv \left(\frac{\sigma}{\theta}\right)^2 + \tau^2 = k^2 \tag{8}$$

where θ is a constant, and k is the yield stress in pure shear. For $\theta = \sqrt{3}$ Eq. (8) corresponds to the von Mises (distortion energy) yield condition and for $\theta = 2$ Eq. (8) corresponds to the Tresca (maximum shear stress) yield condition. If isotropic work-hardening is assumed then there is a one to one correspondence between k and the plastic work W^p. The plastic work rate W_t^p is given by

$$W_t^p = \sigma\varepsilon_t^p + \tau\gamma_t^p \tag{9}$$

From Eqs. (7), (8), and (9) and the relation $W_t^p = \frac{dW^p}{dk} k_t$ the function $\dot{\lambda}$ is found to satisfy

$$\dot{\lambda} = \frac{k_t}{2k^2} \frac{dW^p}{dk} \tag{10}$$

The function $W^p(k)$ can be determined from the stress-strain curve for a simple tension test or a pure shear test. For this, let $\sigma = f(\varepsilon)$ be the stress-strain curve in simple tension. An increment in stress $d\sigma$ is related to the elastic strain increment $d\varepsilon^e$ and the plastic strain increment $d\varepsilon^p$ by

$$d\sigma = f'(\varepsilon)[d\varepsilon^e + d\varepsilon^p] \tag{11}$$

Substituting $d\varepsilon^e = d\sigma/E$ and $d\varepsilon^p = dW^p/\sigma$ in Eq. (11) and regarding the slope of the stress-strain curve (i.e. $f'(\varepsilon)$) as a function of the stress σ, say $g(\sigma)$, we obtain

$$d\sigma = g(\sigma)[\frac{d\sigma}{E} + \frac{dW^p}{\sigma}] \tag{12}$$

For simple tension the yield condition, Eq. (8), reduces to $\sigma = \theta k$. Using the latter relation in Eq. (12) we obtain the following first order differential equation for the function $W^p(k)$.

$$\frac{dW^p}{dk} = \theta^2 k \left(\frac{1}{g(\theta k)} - \frac{1}{E}\right) \tag{13}$$

Eq. (13) and the initial condition $W^p(\sigma_Y/\theta) = 0$, where σ_Y is the initial yield stress in tension, determine the function $W^p(k)$ corresponding to the stress-strain curve $\sigma = f(\varepsilon)$.

The governing equations are obtained by using Eqs. (5), (6), (7), (8), and (10) to express ε_t and γ_t in Eqs. (1) and (2) in terms of σ, τ, σ_t and τ_t. Thus,

Eqs. (1) and (2) become

$$\frac{1}{E}\sigma_t + H(k)[(\frac{\sigma}{\theta})^2 \sigma_t + \sigma\tau\ \tau_t] = u_x \tag{14}$$

$$\frac{1}{\mu}\tau_t + H(k)[\sigma\tau\ \sigma_t + \theta^2\tau^2\ \tau_t] = v_x \tag{15}$$

respectively, where

$$H(k) = \frac{\frac{dW^p}{dk}}{\theta^2 k^3} \tag{16}$$

If Eq. (8) is used to express k in Eq. (16) in terms of σ and τ then Eqs. (3), (4), (14), and (15) constitute a system of four first order partial differential equations for the four unknown functions σ, τ, u and v.

2. Characteristic Properties of the Equations

The governing system of first order partial differential equations derived in the previous section can be written in the following matrix form

$$L[w] \equiv Aw_t + Bw_x = 0 \tag{17}$$

where w is the vector

$$w = \begin{bmatrix} u \\ \sigma \\ v \\ \tau \end{bmatrix}$$

and A and B are the following symmetric matrices.

$$A = \begin{bmatrix} \rho & 0 & 0 & 0 \\ 0 & \frac{1}{E} + H(\frac{\sigma}{\theta})^2 & 0 & H\sigma\tau \\ 0 & 0 & \rho & 0 \\ 0 & H\sigma\tau & 0 & \frac{1}{\mu} + H\theta^2\tau^2 \end{bmatrix} \qquad B = \begin{bmatrix} 0 & -1 & 0 & 0 \\ -1 & 0 & 0 & 0 \\ 0 & 0 & 0 & -1 \\ 0 & 0 & -1 & 0 \end{bmatrix}$$

The system of equations, Eqs. (17), is a system of quasi-linear, symmetric hyperbolic, partial differential equations of first order. (The theory of such equations is given, for example, in Chapter 5 of Ref. [7]). The characteristic velocities c for Eqs. (17) are the roots of the characteristic equation det. C=0 where $C = (cA-B)$ is the characteristic matrix. The characteristic equation is

$$L(\rho c^2)^2 - (M+N)(\rho c^2) + 1 = 0 \tag{18}$$

where

$$L = \frac{1}{\mu E} + \frac{1}{\mu} H(\sigma/\theta)^2 + \frac{1}{E} H\theta^2\tau^2$$

$$M = \frac{1}{\mu} + H\theta^2\tau^2$$

$$N = \frac{1}{E} + H(\sigma/\theta)^2$$

The roots of Eq. (18) are

$$\rho c^2 = \frac{M + N \pm [(M-N)^2 + 4H^2\tau^2\sigma^2]^{1/2}}{2L} \tag{19}$$

The wave speed, taking the plus sign in Eq. (19), will be denoted by c_f and, taking the minus sign, by c_s; the subscripts f and s denote 'fast' and 'slow' wave speeds respectively. For the elastic case (i.e. H=0) c_f becomes the elastic bar velocity $c_o = (E/\rho)^{1/2}$ and c_s becomes the elastic shear wave velocity $c_2 = (\mu/\rho)^{1/2}$. For the case of longitudinal impact (i.e. τ=0) c_f corresponds to the velocity of longitudinal plastic waves for stresses sufficiently small that $c_f > c_2$; otherwise, c_s corresponds to the velocity of longitudinal plastic waves. For the case of torsional impact (i.e. σ=0) c_s corresponds to the velocity of torsional plastic waves.

In order to study the dependence of the wave speeds on the stress state it is helpful to characterize the stress state (σ,τ) by the associated value

of the yield stress k, from Eq. (8), and an angle ϕ by use of the relations

$$\tau = k \sin \phi \tag{20a}$$

$$\sigma/\theta = k \cos \phi \tag{20b}$$

for which the yield condition, Eq. (8), is identically satisfied. Substituting Eqs. (20) in Eq. (19) we obtain expressions for the wave speeds in terms of k and ϕ. These expressions can be simplified by substituting for H, using Eqs. (16) and (13), and writing the slope of the uniaxial stress-strain curve at $\sigma = \theta k$ (i.e. $g(\theta k)$) as βE where $\beta = \beta(k)$ satisfies $0 \le \beta \le 1$ and decreases monotonically with increasing k. In this way we obtain the following dimensionless form for the wave speeds as functions of β and ϕ.

$$\left(\frac{c}{c_2}\right)^2 = \frac{\tilde{M} + \tilde{N} \pm [(\tilde{M}-\tilde{N})^2 + \tilde{P}]^{1/2}}{2\tilde{L}} \tag{21}$$

where

$$\tilde{L} = 1 + (1/\beta - 1)(\cos^2 \phi + \frac{\theta^2}{2(1+\nu)} \sin^2 \phi)$$

$$\tilde{M} = 2(1+\nu) + (1/\beta - 1)\, \theta^2 \sin^2 \phi$$

$$\tilde{N} = 1 + (1/\beta - 1) \cos^2 \phi$$

$$\tilde{P} = 4(1/\beta - 1)^2\, \theta^2 \sin^2 \phi \cos^2 \phi$$

and ν is Poisson's ratio. The wave speeds c_f and c_s given by Eq. (21) are plotted vs. ϕ in Fig. 2 for fixed values of θ, ν, and β.

For values of ν satisfying $0 \le \nu \le 1/2$ and values of θ satisfying $3 \le \theta^2 \le 4$, the wave speeds c_f and c_s satisfy $c_s \le c_2 \le c_f \le c_o$. Furthermore, for an arbitrary fixed value of ϕ, c_s and c_f decrease monotonically with decreasing β. Also, for a fixed value of β, c_s is monotonically decreasing and c_f is monotonically increasing with increasing ϕ for ϕ in the interval $(0, \pi/2)$.

The characteristic curves, or simply the characteristics, for Eqs. (17) are the four families of curves which satisfy

$$\frac{dx}{dt} = \pm c_f \tag{22a}$$

$$\frac{dx}{dt} = \pm c_s \tag{22b}$$

where c_f and c_s are given by Eq. (19). Since the right sides of Eqs. (22) depend on σ and τ the characteristics can be constructed only after the solution $\sigma(x,t)$ and $\tau(x,t)$ is known.

Associated with the characteristic matrix C, for a characteristic with wave velocity c, is a null vector ℓ which satisfies

$$C\ell = 0 \tag{23}$$

There are four linearly independent null vectors corresponding to the four wave velocities $\pm c_f$ and $\pm c_s$. The null vectors for Eqs. (17) which correspond to positive wave velocities are given by

$$\ell_f^+ = \begin{bmatrix} H\sigma\tau c_f \\ -\rho c_f^2 H\sigma\tau \\ \frac{1}{\rho c_f} - c_f\left(\frac{1}{E} + H(\sigma/\theta)^2\right) \\ \rho c_f^2\left(\frac{1}{E} + H(\sigma/\theta)^2\right) - 1 \end{bmatrix} \qquad \text{for } \frac{dx}{dt} = + c_f \tag{24a}$$

$$\ell_s^+ = \begin{bmatrix} \frac{1}{\rho c_s} - c_s\left(\frac{1}{\mu} + H\theta^2\tau^2\right) \\ \rho c_s^2\left(\frac{1}{\mu} + H\theta^2\tau^2\right) - 1 \\ H\sigma\tau c_s \\ -\rho c_s^2 H\sigma\tau \end{bmatrix} \qquad \text{for } \frac{dx}{dt} = + c_s \tag{24b}$$

in which there is an arbitrary scalar factor. The null vectors ℓ_f^- and ℓ_s^- corresponding to negative wave velocities are obtained from Eqs. (24a) and (24b) respectively by replacing c_f by $-c_f$ and c_s by $-c_s$.

The functions σ, τ, u, and v are continuous across a characteristic, but jumps in their derivatives may occur in the direction of the normal to the characteristic. The jump $[w_n]$ in the normal derivative of the vector w must satisfy $C[w_n] = 0$ so that, in view of Eq. (23), $[w_n]$ is proportional to the corresponding null vector ℓ. Since all components of the null vector are non-zero, except for special cases in which either $H = 0$, $\sigma = 0$, or $\tau = 0$, it follows that in general both longitudinal and torsional motion are associated with each wave speed.

The linear combination of Eqs. (17) given by

$$\ell \cdot L[w] = 0 \tag{25}$$

where the dot denotes the Euclidean inner product, is an interior differential equation on the characteristic associated with the null vector ℓ (Ref. [7] pp. 424-427). Substituting Eqs. (24) in Eq. (25) we obtain the following incremental relations along the characteristics.

$$[1/\rho c_f^2 - (1/E + H(\sigma/\theta)^2)]\,[\rho c_f\, dv - d\tau] + H\sigma\tau[\rho c_f\, du - d\sigma] = 0;\quad \frac{dx}{dt} = + c_f \tag{26a}$$

$$[1/\rho c_s^2 - (1/\mu + H\theta^2\tau^2)]\,[\rho c_s\, du - d\sigma] + H\sigma\tau[\rho c_s\, dv - d\tau] = 0;\quad \frac{dx}{dt} = + c_s \tag{26b}$$

The incremental relations along the characteristics $\frac{dx}{dt} = - c_f$ and $\frac{dx}{dt} = - c_s$ are obtained by replacing c_f by $-c_f$ and c_s by $-c_s$ in Eqs. (26a) and (26b) respectively. These incremental relations along characteristics are used in the next section to obtain simple wave solutions. They are also useful in deriving difference equations for the numerical solution of problems involving arbitrary initial and boundary conditions [8].

3. Simple Wave Solutions

There are two types of simple wave solutions of Eqs. (17); namely, slow simple waves in which the solution is constant along the characteristics $\frac{dx}{dt} = c_s$, and fast simple waves in which the solution is constant along the characteristics $\frac{dx}{dt} = c_f$. Characteristics for these two types of simple waves are shown in Fig. 3.

The solution for slow simple waves can be obtained by examining the computation of the solution at point P in Fig. 3(a) for given constant values of σ, τ, u, and v on the characteristic c_s^o. The solution at point P is computed by integration of Eqs. (26) along the characteristics $\frac{dx}{dt} = + c_f, -, c_f$, and $- c_s$. Since σ, τ, u, and v are constant along c_s^o these three incremental relations can be regarded as three ordinary differential equations. Adding the two equations for the characteristics $+ c_f$ and $- c_f$ gives the following first order ordinary differential equation for σ as a function of τ

$$\frac{d\sigma}{d\tau} = \Psi(\sigma,\tau) \tag{27}$$

where

$$\Psi(\sigma,\tau) = \frac{1/E + H(\sigma/\theta)^2 - 1/\rho c_f^2}{H\sigma\tau} \tag{28a}$$

or, in view of Eq. (18), equivalently

$$\Psi(\sigma,\tau) = \frac{H\sigma\tau}{1/\mu + H\theta^2\tau^2 - 1/\rho c_f^2} \tag{28b}$$

It is convenient to also have expressions for Ψ involving the wave speed c_s instead of c_f. Thus

$$\Psi(\sigma,\tau) = - \frac{1/\mu + H\theta^2\tau^2 - 1/\rho c_s^2}{H\sigma\tau} \tag{28c}$$

or

$$\Psi(\sigma,\tau) = - \frac{H\sigma\tau}{1/E + H(\sigma/\theta)^2 - 1/\rho c_s^2} \tag{28d}$$

From Eq. (28b), Ψ vanishes on the τ-axis, on the initial yield surface, and on the σ-axis in the interval $\sigma_Y < |\sigma| < \hat{\sigma}$ where $\hat{\sigma}$ is the stress for which the slope of the uniaxial stress-strain curve is equal to μ. From Eq. (28a), Ψ is infinite at points on the σ-axis for which $|\sigma| > \hat{\sigma}$. Except at these points, the function $\Psi(\sigma,\tau)$ is continuous and continuously differentiable. Thus, a unique solution of Eq. (27) passes through any point $(\tilde{\sigma},\tilde{\tau})$, except the points where Ψ is infinite. This solution will be denoted by $\sigma = \sigma(\tau; (\tilde{\sigma},\tilde{\tau}))$. The solution through a point $(\tilde{\sigma},\tilde{\tau})$ with $\tilde{\sigma} \neq 0$ cannot intersect the τ-axis because $\sigma = 0$ is a unique solution of Eq. (27). Likewise, the solution through a point $(\tilde{\sigma},\tilde{\tau})$ with $\tilde{\tau} \neq 0$ cannot intersect the σ-axis at values of σ satisfying $|\sigma| > \hat{\sigma}$ because, at such points, $\tau = 0$ is a unique solution of the differential equation $d\tau/d\sigma = 1/\Psi(\sigma,\tau)$. Therefore, the solution of Eq. (27) through an arbitrary point $(\tilde{\sigma},\tilde{\tau})$ must either intersect the initial yield surface or intersect the σ-axis in the interval $\sigma_Y \leq |\sigma| \leq \hat{\sigma}$.

Solutions of Eq. (27), obtained by numerical integration, are shown as solid lines in Fig. 4. For these curves a stress-strain curve representing that of annealed commercially pure aluminum was used. The von Mises yield condition (i.e. $\theta = \sqrt{3}$) was used.

In Fig. 4 there are three types of curves: (a) curves that pass through the point $\sigma = \hat{\sigma}$, $\tau = 0$; (b) curves that intersect the σ-axis in the interval $\sigma_Y < |\sigma| < \hat{\sigma}$; (c) curves that intersect the initial yield surface. Each of the curves, or stress paths, represents a locus of stress states that occur at a section during the passage of a slow simple wave. These stress paths are traversed in the directions indicated by the arrows in Fig. 4. The slopes of the curves in Fig. 4 satisfy the inequality

$$0 \leq \frac{d\sigma}{d\tau} < \frac{\sigma}{\theta^2\tau} \tag{29}$$

and approach the upper limit as the radius of the subsequent yield surface, $[(\sigma/\theta)^2 + \tau^2]^{1/2}$, becomes infinite.

The solution for stresses as functions of x and t for a slow simple wave, centered at the origin, is determined implicitly by the relations

$$\sigma = \sigma(\tau; (\tilde{\sigma},\tilde{\tau})) \tag{30a}$$

$$c_s(\sigma,\tau) = \frac{x}{t} \tag{30b}$$

where $\sigma = \sigma(\tau; (\tilde{\sigma},\tilde{\tau}))$ is the stress path for the slow simple wave, and the function $c_s(\sigma,\tau)$ is given by Eq. (19). In order for this slow simple wave solution to be valid, however, the wave velocity c_s must decrease monotonically as the stresses σ and τ increase along the curve $\sigma = \sigma(\tau; (\tilde{\sigma},\tilde{\tau}))$. To show that this is the case it is convenient to regard c_s as a function of β and ϕ as in Eq. (21). Then

$$\frac{dc_s}{d\tau} = \frac{\partial c_s}{\partial \beta}\frac{d\beta}{dk}\frac{dk}{d\tau} + \frac{\partial c_s}{\partial \phi}\frac{d\phi}{d\tau} \tag{31}$$

Recall that $\frac{\partial c_s}{\partial \beta}$ is positive and $\frac{\partial c_s}{\partial \phi}$ is negative (see Fig. 2). From the condition that the stress-strain curve is concave downward $d\beta/dk$ is negative. The result that $d\sigma/d\tau$ satisfies inequality (29) insures that $dk/d\tau$ and $d\phi/d\tau$ are positive. Consequently, $dc_s/d\tau$ is negative and the simple wave solution is valid.

The slow simple wave solution is completed by determining the velocities u and v associated with each point on the stress path $\sigma = \sigma(\tau; (\tilde{\sigma},\tilde{\tau}))$. For this, use is made of the two ordinary differential equations which, in addition to Eq. (27), result from integrating Eqs. (26) along the characteristics $\frac{dx}{dt} = + c_f$, $- c_f$, and $- c_s$ in Fig. (3a). These two equations can be written as

$$\frac{dv}{d\tau} = - \frac{1}{\rho c_s} \tag{32a}$$

$$\frac{du}{d\sigma} = - \frac{1}{\rho c_s} \tag{32b}$$

Since the right side of Eqs. (32) is a known function of σ and τ the change in u and v as the stress state varies along the path $\sigma = \sigma(\tau; (\tilde{\sigma},\tilde{\tau}))$ can be obtained by quadrature.

The change in strain with the passage of a slow simple wave can be obtained by integration of the strain rates, Eqs. (14) and (15), with respect to time, along the path $\sigma = \sigma(\tau; (\tilde{\sigma},\tilde{\tau}))$. Making use of Eqs. (27) and (28), we can write the equations governing the change in strain in the following form

$$\frac{d\varepsilon}{d\sigma} = \frac{1}{\rho c_s^2} \tag{33a}$$

$$\frac{d\gamma}{d\tau} = \frac{1}{\rho c_s^2} \tag{33b}$$

from which the strains can be obtained by quadrature. An interesting consequence of Eqs. (33) is that in slow simple wave regions

$$\frac{d\varepsilon}{d\gamma} = \frac{d\sigma}{d\tau} \tag{34}$$

That is, the direction of the total strain-rate vector coincides with that of the stress-rate vector.

The solution for fast simple waves is obtained in the same way as was the solution for slow simple waves. Integration along the three characteristics in Fig. 3b yields the following differential equation for the stress path for fast simple waves

$$\frac{d\sigma}{d\tau} = -\frac{1}{\Psi(\sigma,\tau)} \tag{35}$$

where $\Psi(\sigma,\tau)$ is the same as in Eq. (28). Comparison of Eqs. (35) and (27) reveals that the stress paths for fast simple waves are orthogonal to the stress paths for slow simple waves. The former are shown as dashed lines in Fig. 4. As these

stress paths are traversed from left to right the wave speed c_f decreases monotonically from c_o to c_2. The equations determining the changes in velocities for fast simple waves, analogous to Eqs. (32), are

$$\frac{du}{d\sigma} = -\frac{1}{\rho c_f} \tag{36a}$$

$$\frac{dv}{d\tau} = -\frac{1}{\rho c_f} \tag{36b}$$

The equations for computing the changes in strains are

$$\frac{d\varepsilon}{d\sigma} = \frac{1}{\rho c_f^2} \tag{37a}$$

$$\frac{d\gamma}{d\tau} = \frac{1}{\rho c_f^2} \tag{37b}$$

From Eqs. (37), the directions of the total strain-rate vector and the stress-rate vector also coincide for fast simple waves.

4. Solution for Step-Loading of a Semi-Infinite Tube

Solutions for a variety of step-loading problems for a semi-infinite tube can be obtained by appropriate combinations of slow and fast simple wave solutions, constant state solutions, and waves of strong discontinuity (i.e. waves across which jumps in stress and velocity occur). Jumps in σ and u can occur only across a wave front with speed c_o; jumps in τ and v can occur only across a wave front with speed c_2. From conservation of momentum these jumps must satisfy

$$[\sigma] = -\rho c_o [u] \quad \text{for } \frac{dx}{dt} = c_o \tag{38a}$$

$$[\tau] = -\rho c_2 [v] \quad \text{for } \frac{dx}{dt} = c_2 \tag{38b}$$

where square brackets denote the jump in the enclosed quantity.

As an example, we consider the case of a tube initially at rest and unstressed which, at the end $x = 0$, is simultaneously subjected to a constant normal stress σ_o and a constant shear stress τ_o. That is, we seek a solution of Eqs. (17) in the region $0 \leq x \leq \infty$, $0 < t < \infty$ which satisfies the initial conditions

$$u(x,0) = \sigma(x,0) = v(x,0) = \tau(x,0) = 0 \tag{39}$$

and the boundary conditions

$$\sigma(0,t) = \sigma_o \qquad 0 < t < \infty \tag{40a}$$

$$\tau(0,t) = \tau_o \qquad 0 < t < \infty \tag{40b}$$

in which σ_o and τ_o are constants satisfying

$$(\sigma_o/\theta)^2 + \tau_o^2 \geq (\sigma_Y/\theta)^2 \tag{41}$$

where σ_Y is the initial yield stress in simple tension.

For this problem there are three types of wave solutions as shown in Figs. 5(a), 5(b), and 5(c); which type results in a given case depends on the values of σ_o and τ_o. Figs. 5(a), 5(b), and 5(c) correspond to the cases when σ_o and τ_o are such that the point (σ_o,τ_o) in Fig. 4 is intersected by solutions of Eq. (27) of types (a), (b), and (c), respectively. Double parallel lines in Fig. 5 represent wave fronts across which jumps in stress and velocity occur. For case (a) the stress wave behavior is as follows: σ jumps to σ_Y across the wave front propagating with a speed c_o; σ increases across the fast simple wave region to $\hat{\sigma}$, according to the von Kármán solution, while τ remains zero; σ and τ increase across the slow simple wave region, following stress path (a) in Fig. 4, until the stress state $\sigma = \sigma_o$, $\tau = \tau_o$ is reached; σ and τ are constant in the constant state region. Case (b) differs from case (a) only in that the fast simple wave

solution terminates when the stress σ reaches the stress, say σ_b, at which the stress path (b) in Fig. 4 intersects the σ-axis. A constant state region with $\sigma = \sigma_b$, and $\tau = 0$ separates the fast and slow simple waves in Fig. 5(b). In case (c) σ jumps to σ_c (see Fig. 4) across the wave front $x = c_o t$; τ jumps from 0 to τ_c across the wave front $x = c_2 t$; σ and τ increase across the slow simple wave region, following stress path (c), to the stress state $\sigma = \sigma_o$, $\tau = \tau_o$. The particle velocities u and v for these three causes can be obtained from the solution for stresses by use of Eqs. (32), (36), and (38).

As a second example we consider a case which differs from the first example only in that the tube is initially stressed statically by a shear stress τ_s which exceeds the initial proportional limit of the material. In this example the final shear stress will again be denoted by τ_o so the jump in shear stress at $t = 0$ is $\tau_o - \tau_s$. The solution for this case can be read from Figs. 6(a) and 6(b); σ increases and τ decreases across the fast simple wave region, following the stress path ab, to the stress state $\sigma = \sigma_1$, $\tau = \tau_1$; there is a constant state region with $\sigma = \sigma_1$, $\tau = \tau_1$ for $c_s(\sigma_1,\tau_1) < \frac{x}{t} < c_f(\sigma_1,\tau_1)$; σ and τ follow the stress path bc as they increase across the slow simple wave region to the final stress state (σ_o,τ_o).

This second example exhibits the unexpected result that the shear stress at any cross-section would first decrease due to the passage of a fast simple wave. It should be possible to carry out experiments that would either verify or refute such a prediction.

A case for which the solution exhibits an even more unexpected behavior is the case where the tube is initially stressed by a tensile stress σ_s and then subjected to step-loading such that the final stress state (σ_o,τ_o) lies outside the yield surface through the point $(\sigma_s,0)$. That is, σ_o and τ_o satisfy

$$(\sigma_o/\theta)^2 + \tau_o^2 > (\sigma_s/\theta)^2 \qquad (42)$$

The solution for this case is shown in Fig. 7. Unloading occurs at the wave front $x = c_o t$ where the normal stress falls to σ_1; τ jumps to τ_1 across the wave front $x = c_2 t$; σ and τ follow the stress path cd as they increase across the slow simple wave region to the final stress state (σ_o, τ_o). In this case the magnitude of the jumps at the two wave fronts clearly depends strongly on the assumption that the subsequent yield surface for tension followed by torsion can be located by the theory of isotropic work-hardening. However, in static tests the subsequent yield surface ordinarily agrees better with the assumption that the yield surface translates in the direction of the initial tensile stress than it does with the assumption of isotropic work-hardening [9]. Therefore, the theoretical predictions in this case probably do not agree well with what would be observed experimentally.

So far solutions have been given for step-loading of tubes subjected to either an initial shear stress $\tau = \tau_s$ or an initial normal stress $\sigma = \sigma_s$. The solution for the case of an arbitrary initial stress state $\sigma = \sigma_s$, $\tau = \tau_s$ can clearly be obtained, without difficulty, using the techniques already established here.

The solutions given here are also valid for the case of combined longitudinal and torsional impact in which the velocities, instead of the stresses, are prescribed at $x = 0$. For given values of prescribed velocities $(\tilde{u}_o, \tilde{v}_o)$ the corresponding stresses at the impact face $(\tilde{\sigma}_o, \tilde{\tau}_o)$ can be obtained by interpolation from a network of contours of constant values of u_o and v_o as shown in Fig. 8. In Fig. 8 a contour u_o = constant represents the locus of applied stresses (σ_o, τ_o) for which the longitudinal velocity at the impact end is u_o. The contours v_o = constant have an analogous interpretation. These contours are obtained by first determining several stress paths for slow simple waves as shown in Fig. 4 and then computing the particle velocities along these paths by numerical integration of Eqs. (32). The contours are then plotted by connecting points on the various stress paths for which the velocities are the same.

Acknowledgment

The author would like to acknowledge the contribution of Mr. David Vitiello, a graduate student in the Division of Engineering at Brown, who performed the calculations for Fig. 4 and Fig. 8.

Bibliography

1. R. Hill, "The Mathematical Theory of Plasticity," Oxford University Press, London, 1950, pp. 14-52.

2. Th. von Kármán, "On the Propagation of Plastic Deformation in Solids," NDRC Report No. A-29, OSRD No. 365, 1942.

3. H. H. Bleich and I. Nelson, "Plane Waves in an Elastic-Plastic Half-Space Due to Combined Surface Pressure and Shear," presented at the winter meeting of ASME, November 1965, (to appear in the Journal of Applied Mechanics).

4. Kh. A. Rakhmatulin, "On the Propagation of Elastic-Plastic Waves Owing to Combined Loading," Applied Mathematics and Mechanics, (PMM), Vol. 22, 1958, pp. 1079-1088.

5. N. Cristescu, "On the Propagation of Elasto-Plastic Waves for Combined Stresses," Applied Mathematics and Mechanics, (PMM), Vol. 23, 1959, pp. 1605-1612.

6. N. Cristescu, "European Contributions to Dynamic Loading and Plastic Waves," Plasticity, edited by Lee and Symonds, Pergamon Press, London, 1960, pp. 385-442.

7. R. Courant and D. Hilbert, "Methods of Mathematical Physics, Vol. II, Partial Differential Equations," Interscience Publishers, New York, 1962.

8. R. Courant, E. Isaacson, and M. Rees, "On the Solution of Nonlinear Hyperbolic Differential Equations by Finite Differences," Communications on Pure and Applied Mathematics, Vol. 5, 1952, pp. 243-255.

9. H. J. Ivey, "Plastic Stress-Strain Relations and Yield Surfaces for Aluminum Alloys," Journal of Mechanical Sciences, IME, Vol. 3, 1961, pp. 15-31.

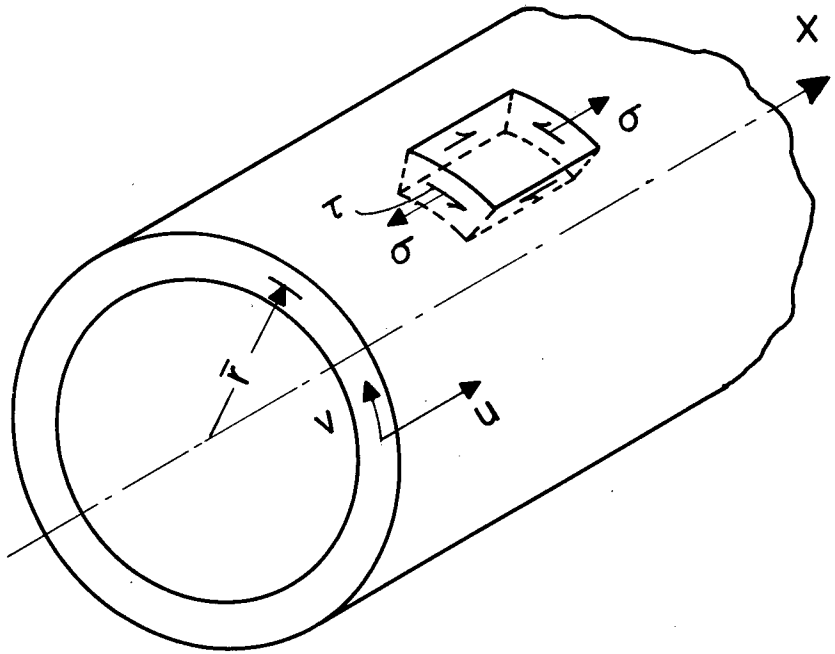

FIG. 1 STRESSES AND VELOCITIES IN THE TUBE

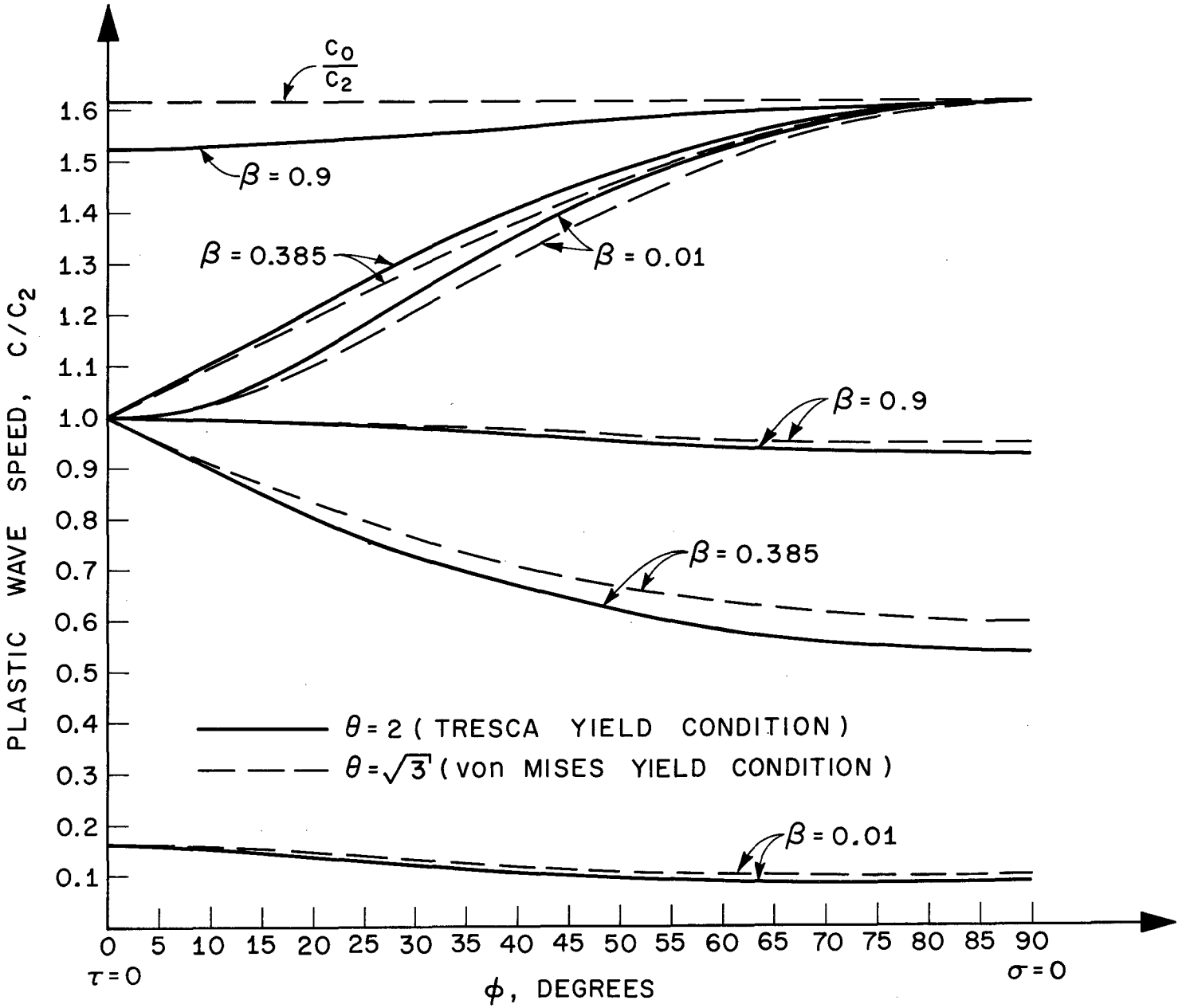

FIG. 2 DEPENDENCE OF PLASTIC WAVE SPEED ON STRESS

(POISSON'S RATIO = 0.3)

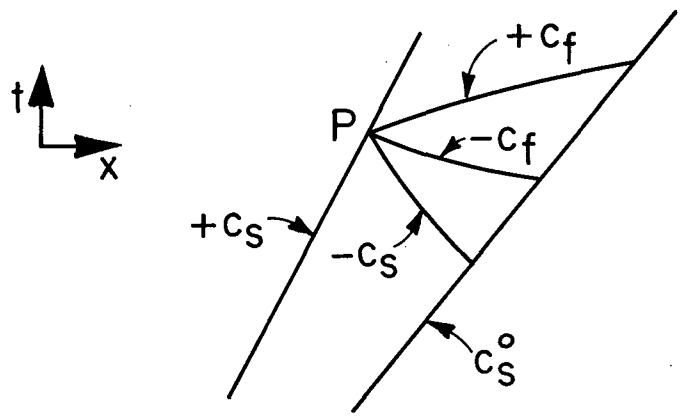

(a) SLOW SIMPLE WAVE

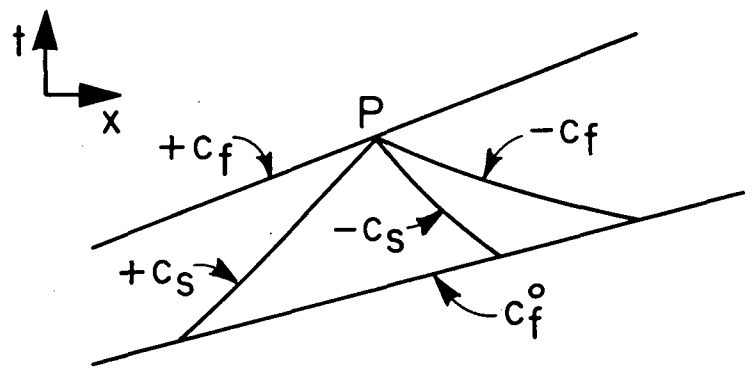

(b) FAST SIMPLE WAVE

FIG. 3 CHARACTERISTICS FOR SIMPLE WAVES

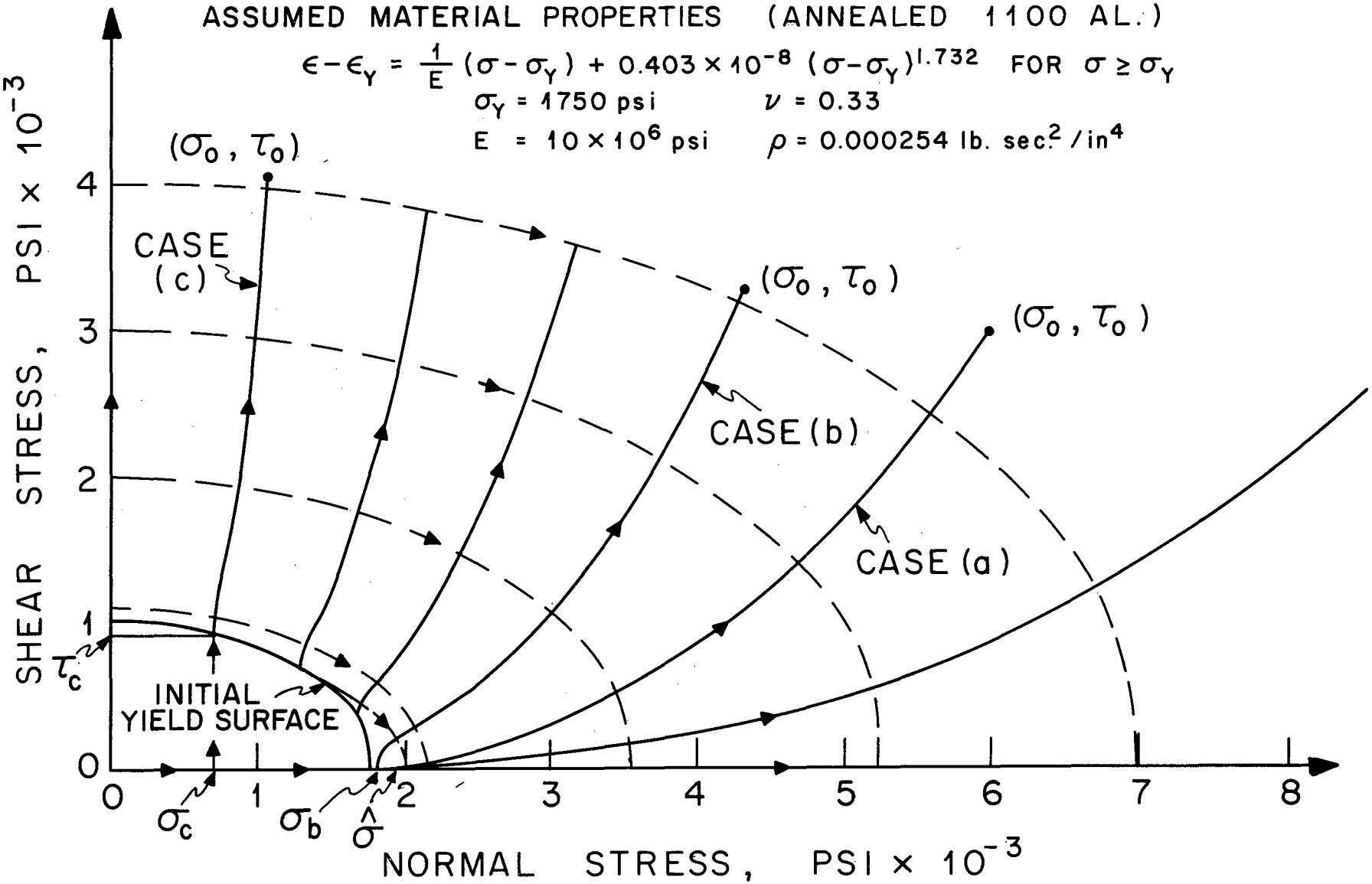

FIG. 4 STRESS PATHS FOR SIMPLE WAVES

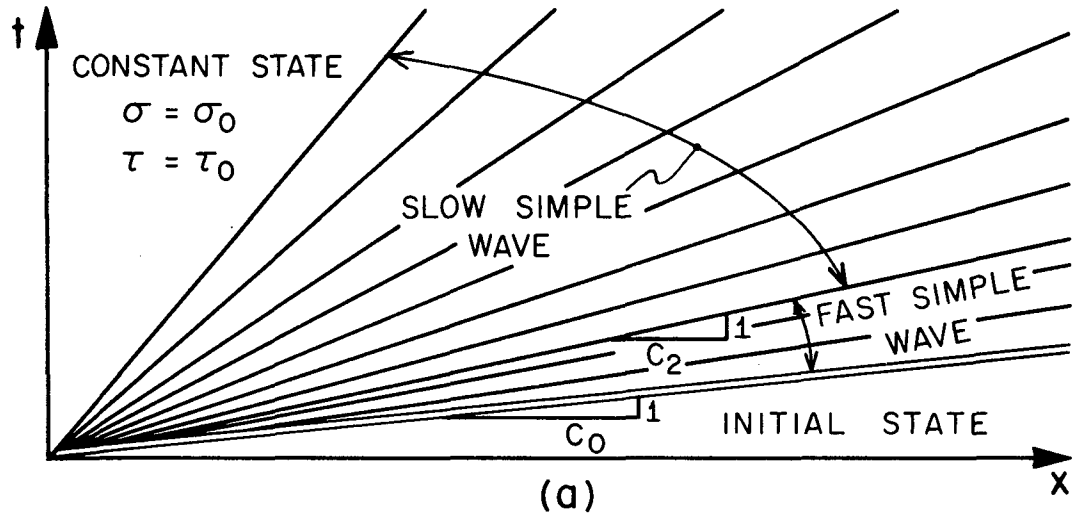

(a)

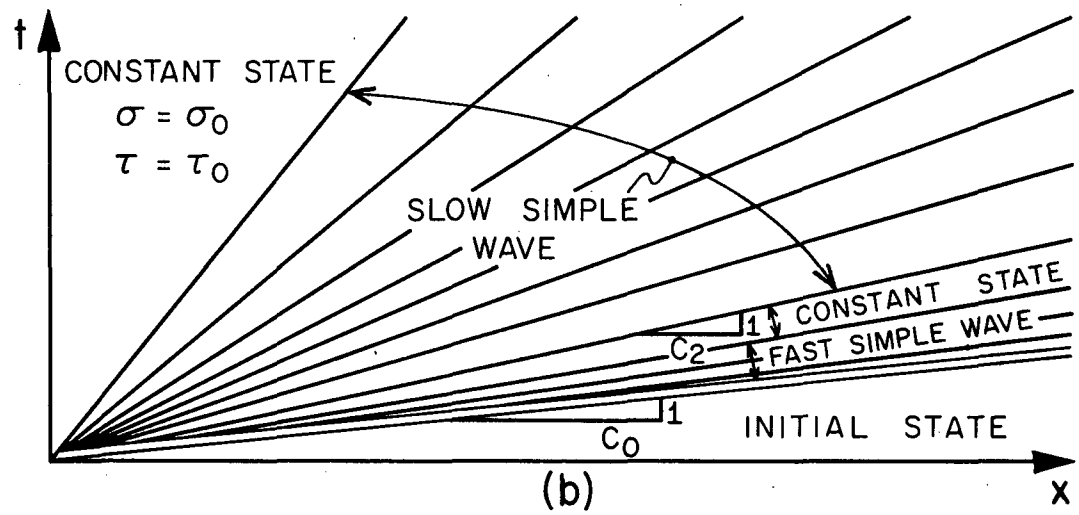

(b)

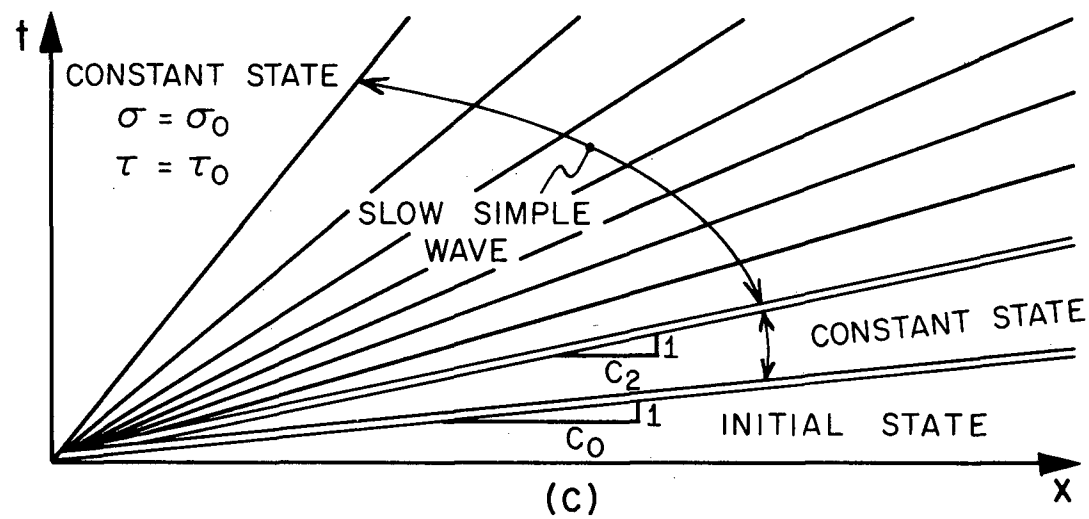

(c)

FIG. 5 CHARACTERISTICS FOR STEP-LOADING

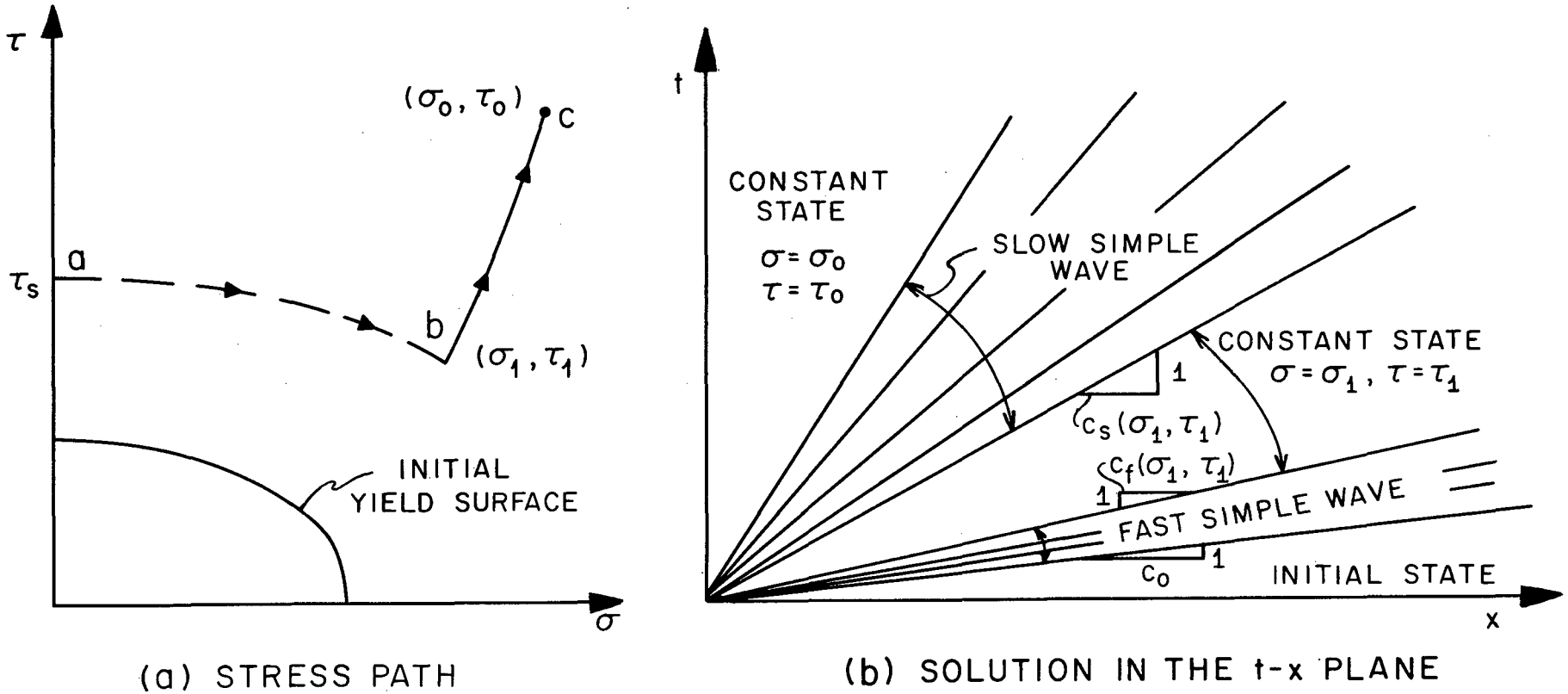

(a) STRESS PATH

(b) SOLUTION IN THE t-x PLANE

FIG. 6 SOLUTION FOR STEP-LOADING OF A PRE-TWISTED TUBE

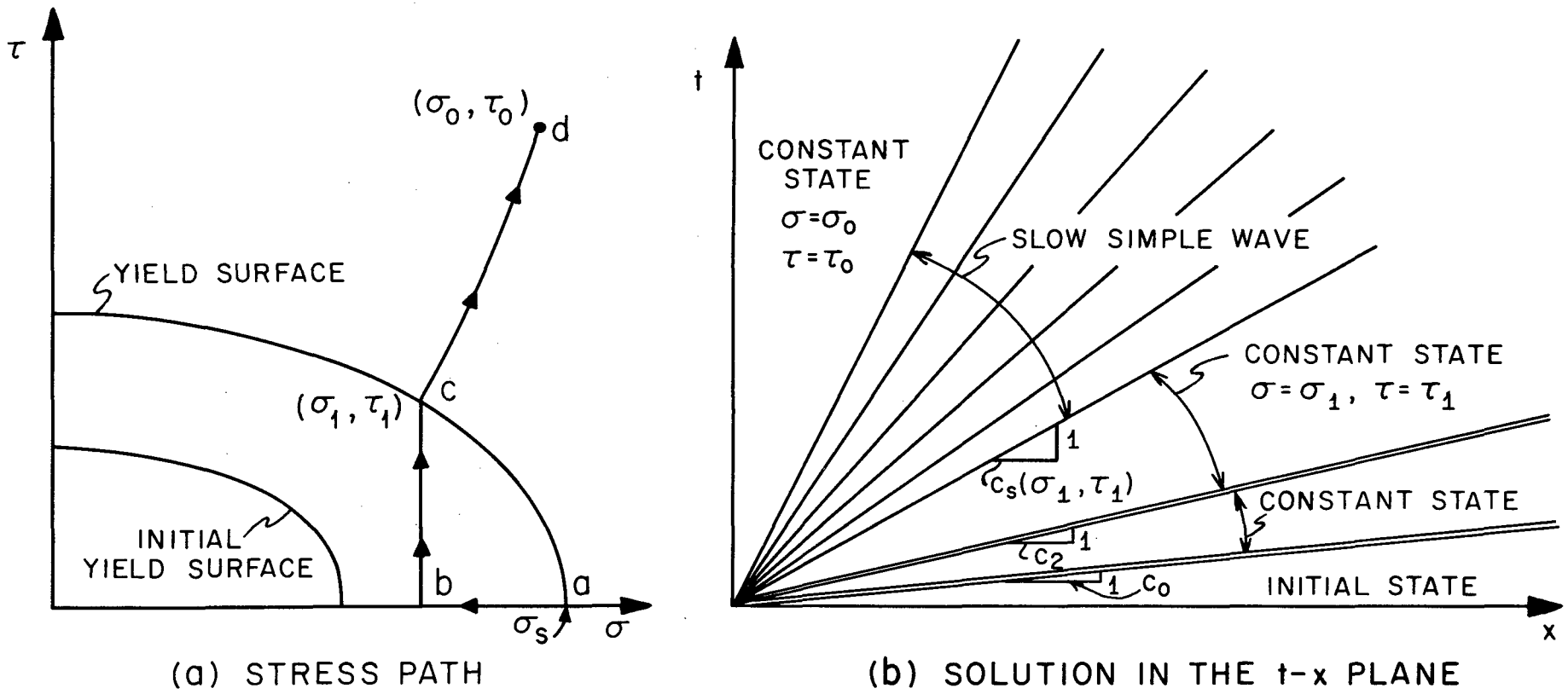

FIG. 7 SOLUTION FOR STEP-LOADING OF A PRE-TENSIONED TUBE

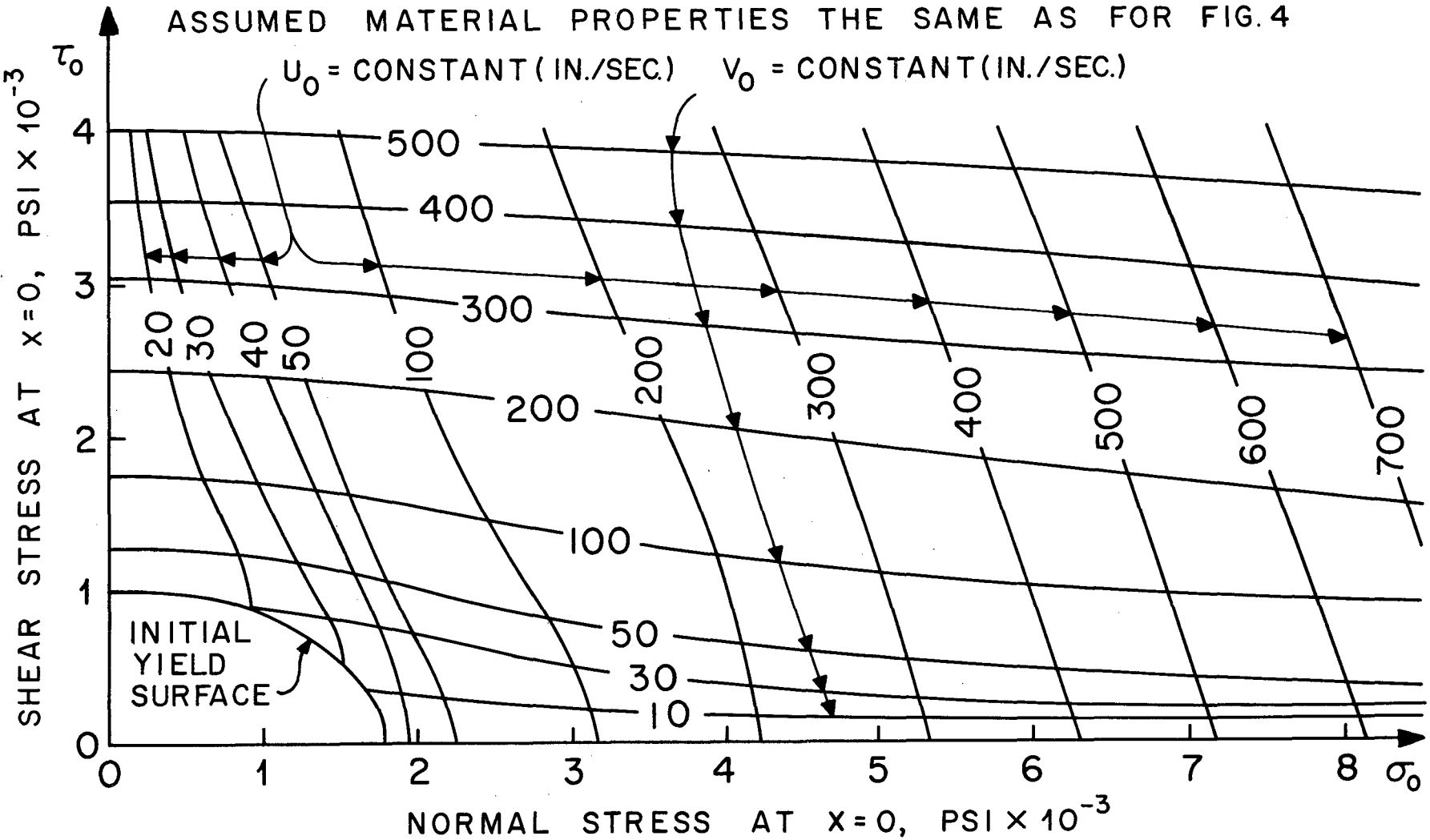

FIG. 8 RELATIONSHIP BETWEEN THE PARTICLE VELOCITIES AND THE STRESSES AT THE IMPACT FACE